

**RECONFIGURABLE ANTENNAS EMBEDDED IN STRUCTURAL
COMPOSITES**

An Undergraduate Research Scholars Thesis

by

DIANA LAU

Submitted to the Undergraduate Research Scholars program at
Texas A&M University
in partial fulfillment of the requirements for the designation as an

UNDERGRADUATE RESEARCH SCHOLAR

Approved by Research Advisor:

Dr. Gregory Huff

May 2018

Major: Electrical Engineering

TABLE OF CONTENTS

	Page
ABSTRACT.....	1
ACKNOWLEDGMENTS	2
NOMENCLATURE	3
CHAPTER	
I. INTRODUCTION	4
Statement of research objective	4
Motivation for research.....	4
II. BACKGROUND	5
Aperture coupled patch antenna and variations	5
Aperture coupled patch antenna model.....	7
Reconfiguration mechanisms.....	8
III. METHODS	11
Base design	11
Parametric studies	13
Final aperture coupled microstrip fed antenna design	16
Fabrication process	18
Reconfiguration study.....	21
IV. RESULTS	24
Fabricated antenna and results	24
Radiation patterns	26
V. CONCLUSION.....	29
Summary	29
Future Work	29
REFERENCES	30
APPENDIX.....	31

ABSTRACT

Reconfigurable Antennas Embedded in Structural Composites

Diana Lau

Department of Electrical and Computer Engineering
Texas A&M University

Research Advisor: Dr. Gregory Huff

Department of Electrical and Computer Engineering
Texas A&M University

Reconfigurable microstrip patch antennas are useful in many applications including satellite communications, navigation, radar, and radio. The purpose of this project is to design a reconfigurable antenna to be embedded in a structural composite for an autonomous vehicle. The antenna is a derivative of an aperture coupled microstrip antenna. It is designed using ANSYS Electromagnetics Desktop software and optimized in simulation by studying how various parameters affect its performance, such as the dimensions of the antenna patch and aperture. In this research project, the antenna is designed to operate at 2.4 GHz. The prototype antenna is fabricated on FR4 epoxy material using a milling machine and tested with a network analyzer and in an anechoic chamber. After analyzing the experimental and simulation results, the design process is reiterated to achieve the best electromagnetic performance. A major benefit to reconfigurable antennas is the ability to accommodate changing operating requirements. Solid state reconfiguration mechanisms (RF PIN diodes, RF MEMs, and varactors) are explored to reversibly configure operating frequencies. Moreover, the reconfiguration of the antenna would provide advantages such as reversible changes, additional functionality, and flexibility for many applications at a low cost.

ACKNOWLEDGEMENTS

I would like to thank Dr. Huff for extending the wonderful opportunity to be a part of his research group. His continual guidance and positive support has helped me move forward to achieve my research goals. I also want to thank the graduate students within Huff Research Group for their kindness, openness, and assistance in the pursuit of my project. Thank you to all my family and friends for their love and support.

NOMENCLATURE

AFRL	Air Force Research Laboratory
ANSYS	Analysis System
DXF	Drawing Interchange Format
RF MEMS	Radio Frequency Microelectromechanical Systems
RF PIN	Radio Frequency Positive Intrinsic Negative
VNA	Vector Network Analyzer
VSWR	Voltage Standing Wave Ratio

CHAPTER I

INTRODUCTION

Statement of research objective

The objective of this project is to design a pattern-reconfigurable printed antenna that is structurally embedded into a composite as a component of an autonomous ground vehicle for AFRL. Parametric studies are completed to gain insight on designing an aperture coupled microstrip patch antenna. Various reconfiguration techniques are explored to change the operating frequency of the antenna.

Motivation for research

In modern applications, reconfigurable antennas and microstrip patch antennas are useful in wireless communications because of its ability to radiate more than one pattern at different frequencies. With reconfiguration mechanisms, the antenna can accommodate increased functionalities and adapt to different environments. One advantage in reconfigurable antennas is the ability to control its electromagnetic behaviors remotely. This is why reconfigurable antennas are useful in space communication. Secondly, the implementation of a reconfiguration mechanism helps reduce the complexity of the hardware. A single antenna can be reconfigured to provide various electromagnetic performances in terms of frequency, polarization, radiation pattern, or a combination of these properties [4]. In addition, utilizing a microstrip patch antenna design is advantageous for an autonomous vehicle, because it provides conformability to a shaped surface and ease in fabrication at a low cost.

CHAPTER II

BACKGROUND

Aperture coupled patch antenna and variations

The aperture coupled antenna is useful in wireless communication and space applications. It is commonly fed by microstrip transmission lines and coaxial probes [3]. The objective of this research focuses on microstrip lines. The idea of isolating the microstrip line and patch antenna was introduced in 1985 [3]. Isolating the patch and microstrip with a thick substrate material in between allows for independent optimization of electromagnetic behaviors [7]. In addition, a microstrip patch antenna offers many advantages including low profile, ease of fabrication, compatibility with integrated circuits, and conformability to a shaped surface [7].

An advantage of aperture coupled antennas is that it does not require a direct connection between the feedline and the antenna. As described earlier, a coaxial probe is one common way to feed an antenna. Probe fed antennas require a direct connection between the patch and feedline. This causes an undesirable distortion in the electric field between the patch and the ground plane [3]. In contrast, the microstrip feedline depicted in Figure 1 induces a current in the ground slot, which is used to control the coupling levels [2]. This helps to eliminate spurious radiation. The ground slot is on a separate substrate from the microstrip feedline which helps provide more substrate space for additional antenna elements and reconfiguration mechanisms [7]. In addition, radiation can be optimized by independently selecting the thickness and dielectric constant of each substrate [7]. The ability to select the material characteristics of each layer and control the coupling level through the ground slot make the aperture coupled patch antenna desirable.

The aperture coupled antenna is a multilayer structure which includes a metallic patch, ground slot plane, and a microstrip line (Figure 1). A disadvantage of aperture coupled antennas is its increased complexity in the fabrication of multiple layers. Additionally, aperture coupled microstrip antennas typically have a narrow bandwidth of around 5 to 10 percent [7]. However, there is on-going research which shows positive results in increasing the bandwidth to 50 percent by using stacked patches (Figure 2). Additionally, the multilayer structure of the aperture coupled antenna provides many degrees of freedom in its design. As a result, there are many variations to the basic aperture coupled patch. This research focuses on a single rectangular patch. Other types of radiating elements include circular patches, stacked patches, and thin printed dipoles [7]. Similarly, the slot shape of the aperture impacts the coupling effect between the feedline and the patch. Variations of the slot shape include the dog bone, bow-tie, H-shaped, and the thin rectangular slot [7]. The thin rectangular slot is implemented in this research because it is the most common aperture shape and provides better coupling compared to the others.

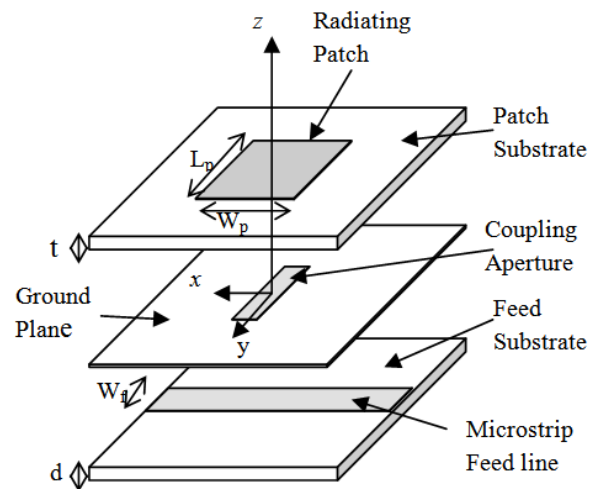


Figure 1. Basic geometry of an aperture coupled microstrip fed patch antenna

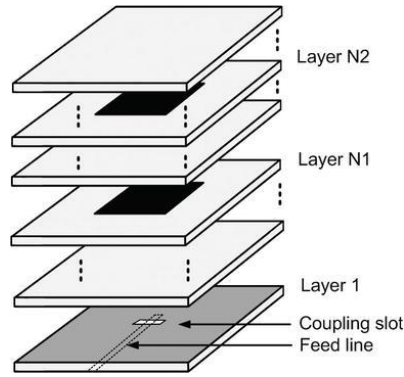


Figure 2. Bandwidth enhancement technique using stacked patches

Aperture coupled patch antenna model

The aperture coupled microstrip fed antenna can be modeled by an equivalent electrical circuit shown in Figure 3. The ground slot or coupling between the feedline and the antenna is represented by an impedance transformer [6]. In terms of the antenna parameters, the turn ratio is determined to be the ratio of the nominal patch width to the slot length [3]. The fringing effects of the patch and the resonance behavior of the ground slot plane are represented by the parallel LC circuit [3]. Finally, the resistor and capacitor components represent the fringing effects of the patch [2]. The fringing fields at the edge of the patch antenna are responsible for the radiation. Generally, the fringing electric fields increase as the antenna width increases.

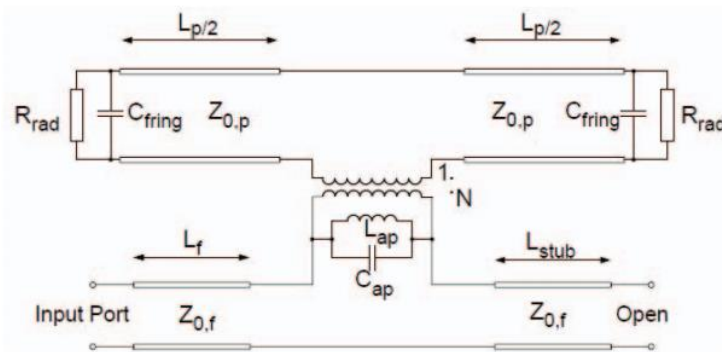


Figure 3. Model of an equivalent circuit for an aperture coupled microstrip patch antenna

Reconfiguration mechanisms

A reconfigurable antenna has inner mechanisms with the ability to alter its fundamental operating characteristics in a controlled and reversible manner. Reconfigurable antennas are useful in telecommunication systems such as mobile devices. For example, antenna configurability allows the antenna to filter out interfering signals, change the operating band, or redirect the antenna radiation pattern [1]. This helps minimize costs and save battery power of a device. The different types of antenna reconfigurations include frequency, radiation pattern, polarization, and compound configuration. The focus of this research is to tune the operating frequency of the antenna. The effective length of the antenna largely determines the operating frequency and bandwidth [1]. There are various techniques that can be used to achieve frequency-reconfigurable antennas, also known as tunable antennas. The four major categories of reconfiguration techniques are electrical, optical, mechanical, and material change [4]. The techniques explored in this research project include the following electrical components: RF MEMS, RF PIN diodes, and varactors.

RF MEMS

Radio frequency micro-electromechanical systems (RF MEMS) are based on mechanical movement of switches to achieve reconfiguration [4]. Switches work by adding or removing length to an antenna element such as the microstrip feedline. Through changing the microstrip feedline length, the antenna exhibits different electromagnetic behaviors. RF MEMS are often applied in satellites, phased arrays, and wireless communications. Advantages of RF MEMS are that it requires low power consumption and helps reduce the mass and volume of electrical equipment [8]. As an example, the reduction in mass and volume significantly reduces the costs

to launch a satellite into space [8]. However, the two main drawbacks of RF MEMS are its high actuation voltage and slow switching speed [8]. It has a low switching speed in the range of 1 to 200 microseconds which may be too slow in some applications [4]. Little research has been done on improving the switching speed because increasing the switching speed results in a higher actuation voltage [8]. As for the requirement of high actuation voltage, previous research shows that improvements come at the expense of the reliability of the device and its switching speed [8]. Therefore, it is likely that the performance of RF MEMS is limited, since the two main drawbacks are linked together.

RF PIN diodes

The radio frequency PIN diode is a solid-state switching mechanism. In comparison to RF MEMS, RF PIN diodes are more compact and have a faster switching speed of 1 to 100 microseconds [4]. Because of its faster switching speed, RF PIN diodes require higher power consumption. The main advantage of RF PIN diodes is the ability to operate at higher frequencies. The PIN diode is a simple passive element and behaves as a current-controlled resistor at radio and microwave frequencies [5]. When the PIN diode is forward biased, RF energy flows. Likewise, when the PIN diode is reverse biased, RF energy does not flow. The electrical models of the forward bias consist of a resistor and inductor in series, while the electrical model of the reverse bias consist of a capacitor and resistor in parallel [5]. Although the PIN diode itself has a simple functionality, the application of the RF PIN diode is challenging for several reasons. One limitation is that it requires to operate at the gigahertz region [5]. Additionally, since the PIN diode is a two-port device, the design must contain both DC

components and the RF signal [5]. Generally, RF PIN diodes require more careful circuit designing, but it offers characteristics that other reconfiguration mechanisms do not.

Varactors

Lastly, varactors are a biased voltage variable capacitor. The main difference between a variable capacitor and the switching mechanisms (RF MEMS and RF PIN diodes) is that the variable capacitor offers a continuous range of values rather than discrete changes when tuning the antenna [1]. The switching mechanisms and varactors can be combined to achieve course and fine tuning [1]. Like RF PIN diodes, varactors provide a fast switching response. By changing the applied bias voltage level, a variable capacitor on the antenna causes the current distribution to change. This effectively alters the length of the microstrip feedline to tune the antenna. An advantage of using varactors is that they can reside on the antenna feedline. As a result, varactors have a minimal effect on the antenna radiation patterns and provide frequency tuning operations without additional interferences [4]. In addition, varactors generally require a small supply of DC voltage and have low resistances. An example of a tuning varactor is the SC-79. The performance characteristic of the SC-79 varactor is illustrated in Figure 4. By applying a small DC voltage of 0 to 5 volts, the potential capacitance value can vary from 0 to 90 picofarads.

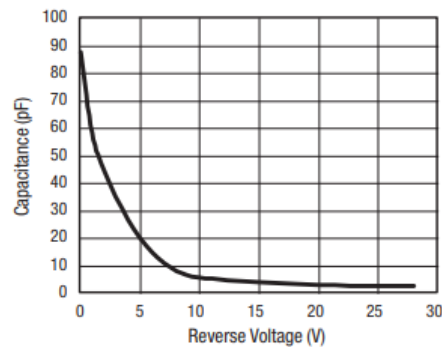


Figure 4. Capacitance vs. Reverse Voltage of the SC-79

CHAPTER III

METHODS

Base design

The target operating frequency of the single aperture coupled antenna matched with a 50-ohm impedance is 2.4 GHz. The first step in the design process of the aperture coupled patch antenna with a microstrip feedline is to start off with a rough estimation of the length and width of the patch and microstrip line. To determine the length and width of the patch, the dielectric constant (ϵ_r) and height are needed. In this specific design, FR4 epoxy is the substrate material. It has a height of 62 mil and a dielectric constant of 4.4. These substrate parameters are used to calculate the length and width of the antenna patch in the following equations:

$$Width = \frac{c}{2f\sqrt{\frac{\epsilon_r+1}{2}}} \quad (1)$$

$$\epsilon_{eff} = \frac{\epsilon_r+1}{2} + \frac{\epsilon_r-1}{2} \left[\frac{1}{\sqrt{1+12\left(\frac{h}{Width}\right)}} \right] \quad (2)$$

$$Length = \frac{c}{2f\sqrt{\epsilon_{eff}}} - 0.824h \left(\frac{(\epsilon_{eff}+0.3)\left(\frac{Width}{h}+0.264\right)}{(\epsilon_{eff}-0.258)\left(\frac{Width}{h}+0.8\right)} \right) \quad (3)$$

Similarly, the substrate parameters determine the width and length of the microstrip feedline. The microstrip feedline is used to impedance match the antenna. Using an electrical length of 90 and characteristic impedance of 50, the microstrip feedline dimensions are calculated based on the following equations:

If $\left(\frac{W}{H}\right) < 1$:

$$\varepsilon_{eff} = \frac{\varepsilon_r+1}{2} + \frac{\varepsilon_r-1}{2} \left[\frac{1}{\sqrt{1+12\left(\frac{H}{W}\right)}} + 0.04 \left(1 - \left(\frac{W}{H}\right)\right)^2 \right] \quad (4)$$

$$Z_0 = \frac{60}{\sqrt{\varepsilon_{eff}}} \ln \left(8 \left(\frac{H}{W}\right) + 0.25 \left(\frac{W}{H}\right) \right) \quad (5)$$

If $\left(\frac{W}{H}\right) > 1$:

$$\varepsilon_{eff} = \frac{\varepsilon_r+1}{2} + \left[\frac{\varepsilon_r-1}{2\sqrt{1+12\left(\frac{H}{W}\right)}} \right] \quad (6)$$

$$Z_0 = \frac{120\pi}{\sqrt{\varepsilon_{eff}} \left(\left(\frac{W}{H}\right) + 1.393 + \frac{2}{3} \ln \left(\left(\frac{W}{H}\right) + 1.444 \right) \right)} \quad (7)$$

To simplify the calculation process, Pasternack's patch antenna and Em Talk's microstrip line calculators were used to estimate the dimensions for the antenna design. The physical length and width for the patch are found to be approximately 29.77 mm and 38 mm. For the microstrip line, the length and width are approximately 3 mm and 17 mm respectively. These design parameters are used in the initial estimation of the patch and microstrip line dimensions. In Figure 5, the simulation results on ANSYS Electronics Desktop show an operating frequency of 2.26 GHz and VSWR at 5.4; however, the desired behavior is to have the operating frequency to be 2.4 GHz with a VSWR at 1 to reduce reflections and maximize the power transmitted. The calculated dimensions provide a rough estimation and starting point for the antenna design.

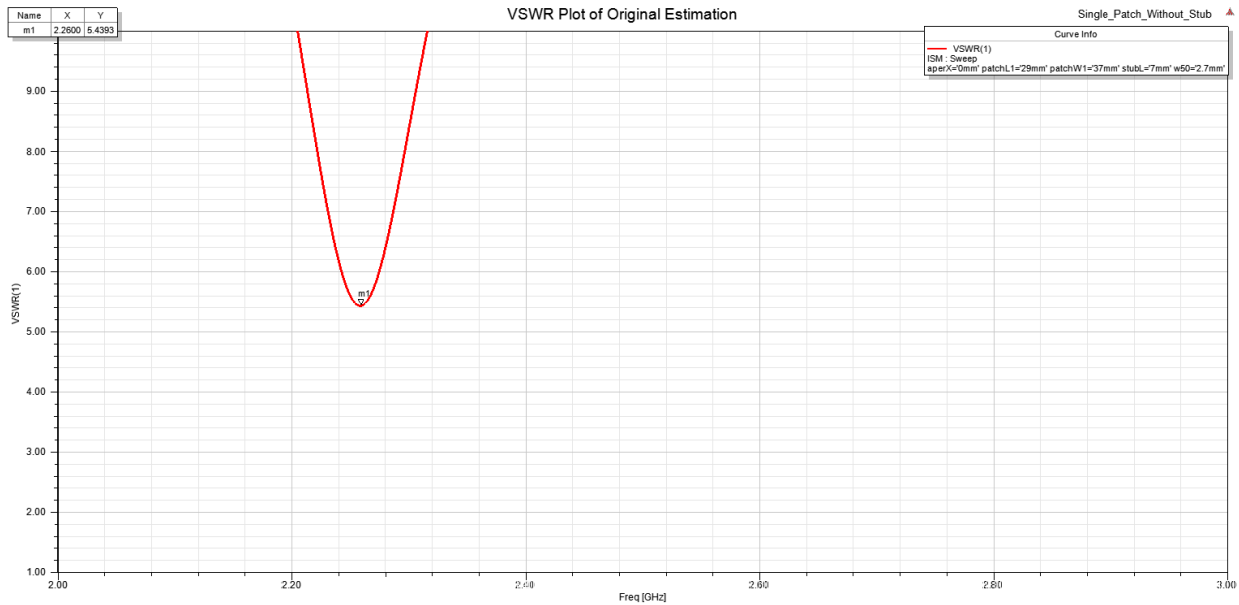


Figure 5. VSWR plot using the calculated dimensions

Parametric studies

The next step is to run parametric studies on different antenna parameters to tune the antenna to the desired operating frequency at 2.4 GHz with a VSWR close to 1. The position of the slot and the dimensions of the patch, microstrip line, and slot are individually examined. The method behind the parametric study is to change one parameter at a time and see how it affects the results. Then, after a few iterations of simulations on ANSYS, the value for the isolated parameter that results in the best electromagnetic performance is selected. This selected value becomes fixed, and the process is repeated for the other parameters until the design operates at the desired frequency of 2.4 GHz. The following patterns are observed from the parametric study.

Length and width of the patch antenna

For the radiating antenna patch, the two adjustable parameters are the length and width, depicted in Figure 6 as W_p and L_p . The length of the patch antenna determines the resonant frequency of the antenna [7]. The length of the patch antenna has an inverse effect on the resonant frequency. As the patch length increases, the operating frequency decreases. Secondly, the width of the patch determines the resonance resistance of the antenna. As the width increases, the resonance resistance decreases [7]. Ideally, the antenna patch width is fixed and does not require large adjustments. Typically, adjustments are made to the length of the patch antenna, because it has a greater effect in shifting the frequency of operation.

Width of the microstrip feedline

The width of the microstrip feedline determines its characteristic impedance. As the width decreases, the characteristic impedance increases. The width of the microstrip line depends on the operating frequency, dielectric constant, and dielectric height. It can be calculated using online microstrip calculators or by the set of microstrip equations (4) through (7) in the previous section. Generally, the width of the microstrip feedline is kept constant, because the characteristic impedance does not change significantly from changes in other parameters.

Length and width of the aperture

The aperture or ground slot determines the amount of coupling between the microstrip line and the radiating antenna patch. The slot length affects the resonant frequency, coupling level, and the back-radiation level [7]. Back-radiation occurs because the aperture radiates in both directions, the upper and lower spaces [6]. An increase in aperture length results in a

decrease in both the operating frequency and the VSWR. A lower VSWR value means that it is better impedance matched and radiates more total power. In comparison to the aperture length, the width of the aperture has a smaller effect on the coupling levels [7]. Ideally, the ratio of the aperture length to width is 1/10 [6]. Typically, the aperture position should be centered to maximize the coupling effects.

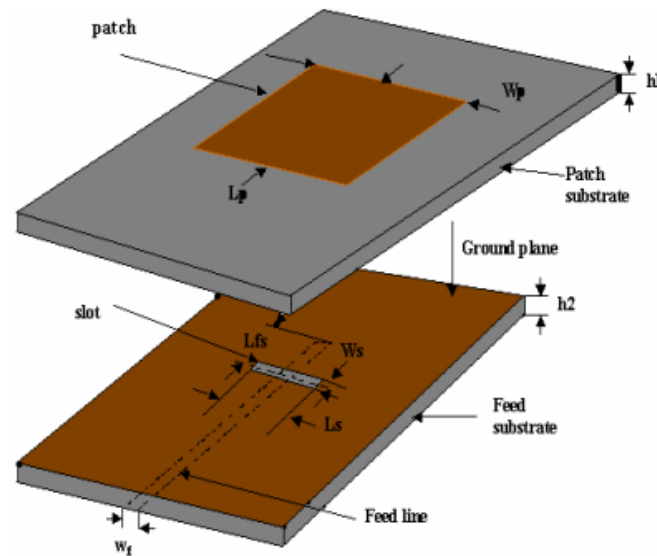


Figure 6. Aperture coupled microstrip patch antenna parameters

Length of the tuning stub

The length of the tuning stub is the length of the feedline that extends after the aperture. This is illustrated in Figure 6 as L_{fs} . This parameter is used to tune the excess reactance of the microstrip feedline [6]. In terms of the smith chart, as the length of the tuning stub decreases, the impedance of the smith chart will move in the capacitive direction [6]. The typical value of the length of the tuning stub is slightly less than $\lambda_g/4$ [7].

Final aperture coupled microstrip fed antenna design

A final antenna design shown in Figure 7 is created using the intuitive knowledge gained from the parametric studies. The final aperture coupled antenna design has the following dimensions shown in Table 1. These dimensions yield a VSWR of 1.07 at 2.4 GHz (Figure 8).

Table 1. Dimensions for aperture coupled microstrip fed antenna design ($\epsilon_r = 4.4$)

Parameter	Value
Substrate Height	62 mils
Patch Length and Width	26.5 mm x 36 mm
Microstrip Width	3 mm
Slot Length and Width	5 mm x 6.4 mm
Stub Length	1.5 mm

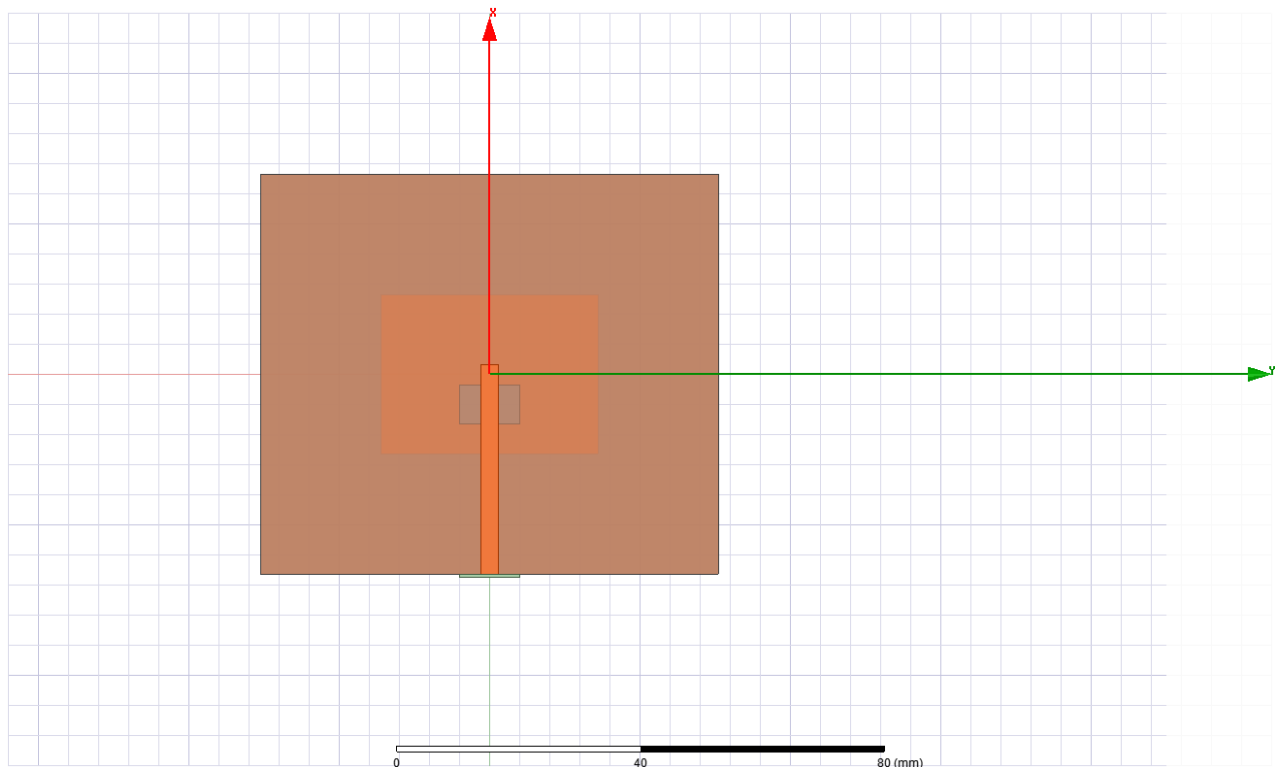


Figure 7. ANSYS model of the aperture coupled microstrip fed patch antenna.

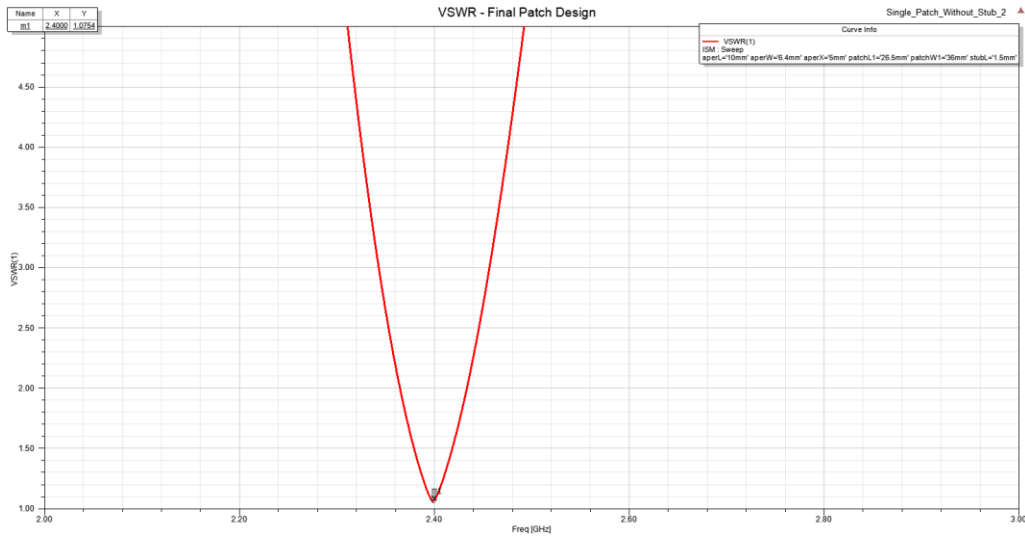


Figure 8. VSWR plot of the final antenna design

The smith chart depicted in Figure 9 shows that at an operating frequency of 2.4 GHz, the antenna is matched to 53.5Ω . This is determined by taking the real part of the impedance and multiplying it by the characteristic impedance. There is a small amount of energy stored since the reactance at 2.4 GHz is nonzero. At 2.4 GHz, the reactance is 0.0265 (Figure 9). At the center of the smith chart, the reactance is zero. This represents maximum power and no reflections.

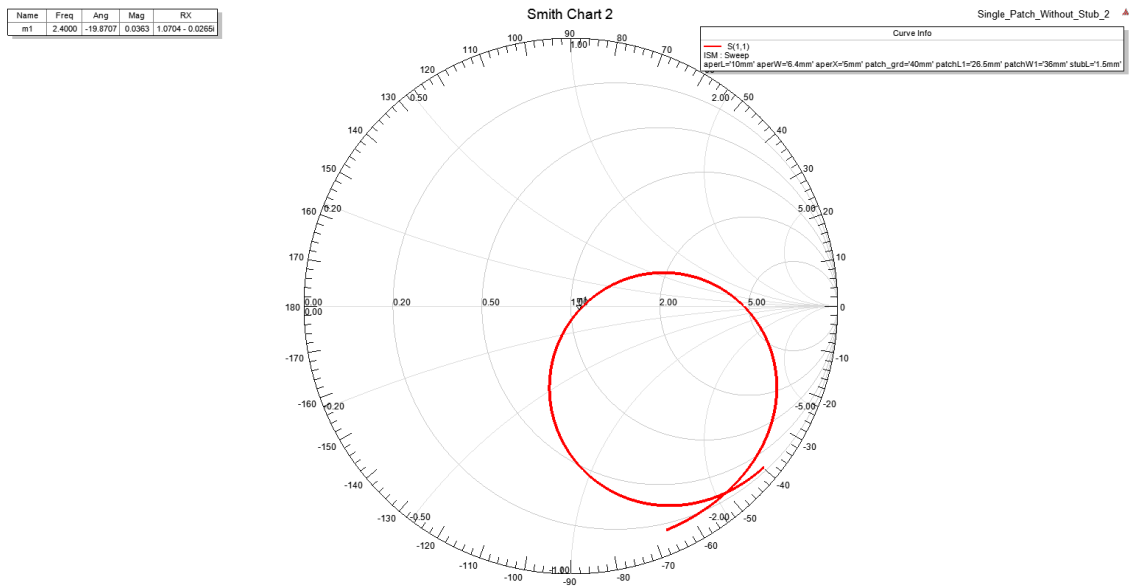


Figure 9. Smith chart of the final antenna design

Fabrication process

From the final aperture coupled antenna design on ANSYS, each layer is then isolated and shifted onto the x-y plane to export each layer as a drawing interchange format, or AutoCAD DXF file. This is done for the patch, microstrip feedline, ground slot plane, and an additional ground slot plane with a notch (Figure 10). A second ground slot plane with a notch is created, because the antenna design requires two 62 mil thick substrates and the only available connector is for a single 62 mil thick substrate (Figures 11). For the microstrip feedline design, two additional small strips were added to connect the three prongs of the SMA connector (Figure 11). The DXF files are then transferred to the Quick Circuit milling machine to fabricate the antenna (Figure 12). Two layers of the antenna is fabricated on a 62 mil thick FR4 epoxy material because of its availability and low cost.

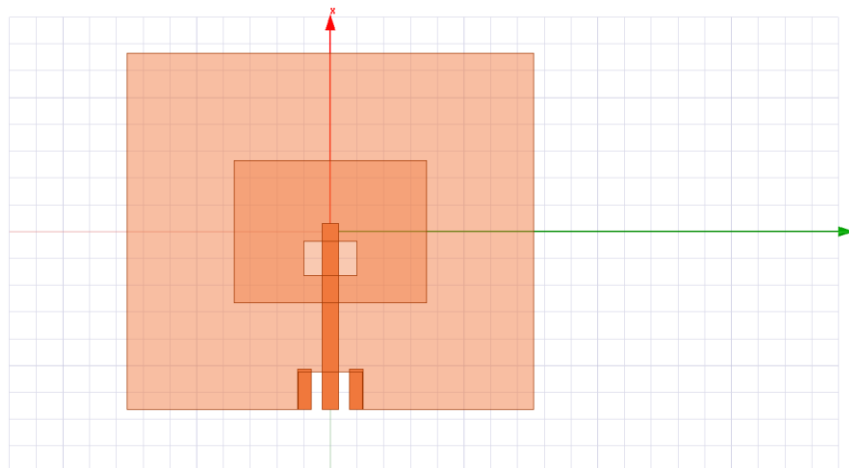


Figure 10. Updated design with additional small strips and a ground plane notch



Figure 11. 62 mil SMA connector for the antenna

The FR4 substrate is placed on the milling machine and secured in place with the milling holes and tape. Three types of milling tools are used to fabricate the antenna. For the first layer, a small milling tool is used to cut the patch shape, and a thicker milling tool is used to trace the patch shape and mill around the patch. The design is mirrored and the FR4 substrate is flipped over to mill the aperture. Finally, a third milling tool is used to cut out the first layer of the antenna. A similar procedure is repeated for the second layer which includes the microstrip line and ground plane slot.

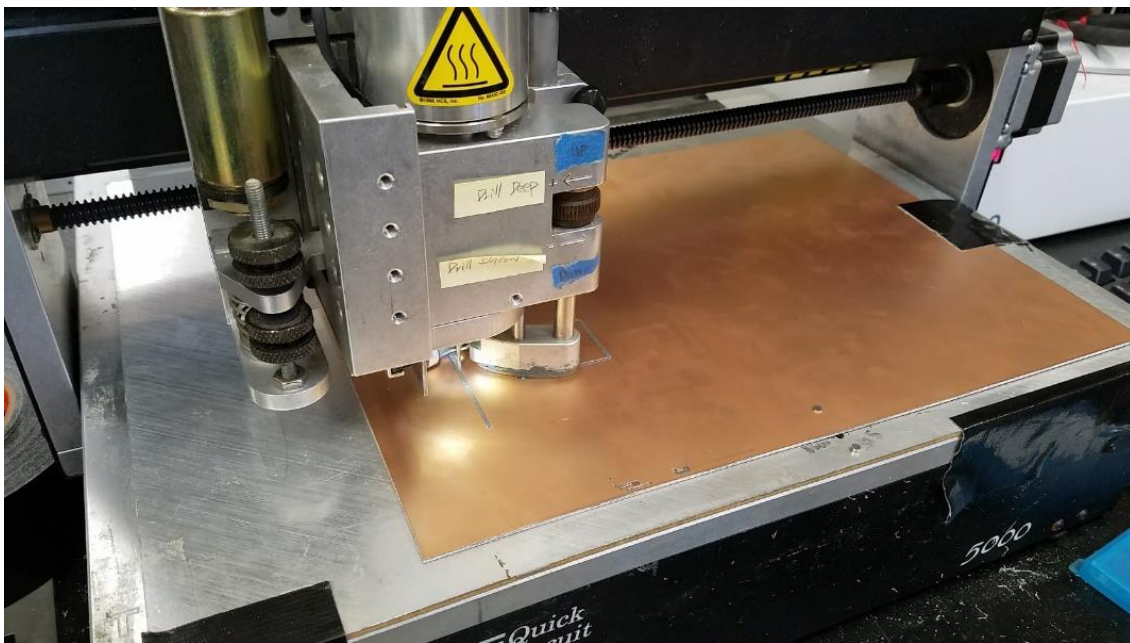


Figure 12. Quick circuit milling machine

The two layers of the antenna are pictured in Figures 13 and 14. The two layers are glued together with the ground planes in the middle. It is secured by clamps and left over night to dry (Figure 15). After the antenna is completely dried, the three-pronged 62 mil SMA connector is carefully soldered onto the microstrip line and the additional two small lines.



Figure 13. Ground plane with slot (left) and microstrip plane (right)

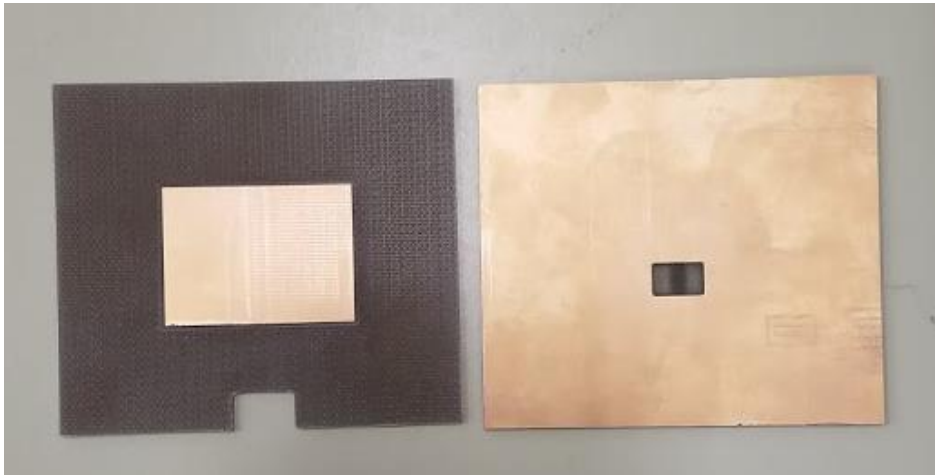


Figure 14. Patch antenna (left) and aperture slot (right)

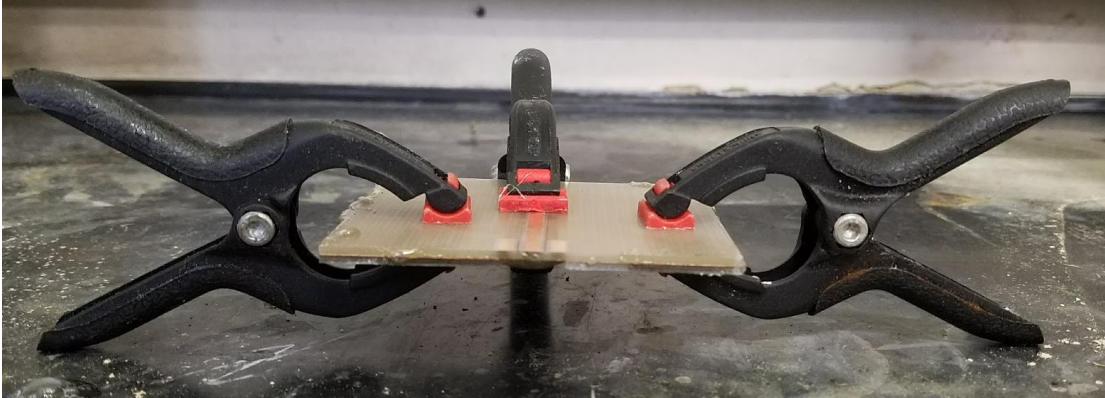


Figure 15. Drying process of attaching the two sheets together

Reconfiguration study

Reconfiguration of the antenna was explored by using stubs to tune and detune the antenna on ANSYS Electronics Desktop. To analyze the tuning of the antenna on ANSYS, a stub is added at the edge of the radiating patch (Figure 16). The stub length is varied from 0 mm to 10 mm in increments of 2.5 mm. The frequency tuning with stubs is analyzed on an aperture coupled antenna designed at 2.442 GHz using the material Rogers AD250C ($\epsilon_r = 2.5$). The design parameters in Table 2 for the aperture coupled antenna yield a VSWR of 1.07.

Table 2. Dimensions for aperture coupled microstrip fed antenna design ($\epsilon_r = 2.5$)

Parameter	Value
Substrate Height	20 mils
Patch Length and Width	36 mm x 45 mm
Microstrip Width	1.38 mm
Slot Length and Width	0.5 mm x 1 mm
Stub Length	10 mm

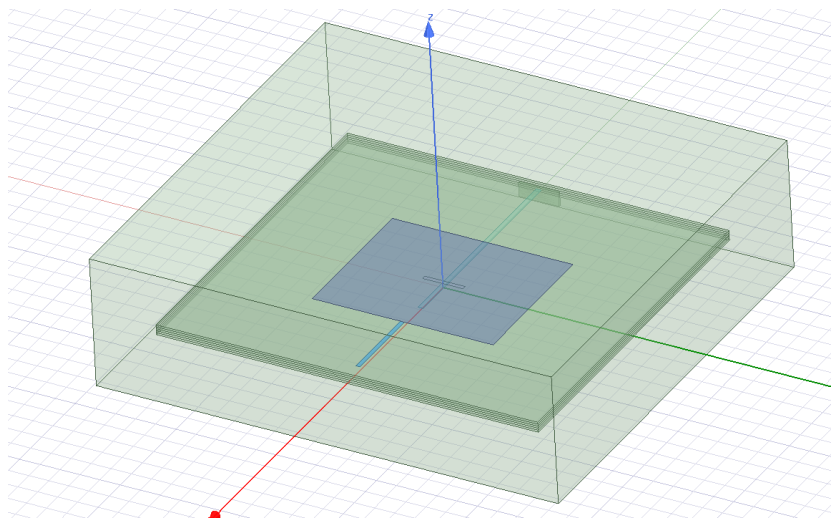


Figure 16. Aperture coupled patch antenna with a tuning stub attached

As the stub length increases, the operating frequency is shifted to the left and the aperture coupled patch antenna is detuned. When the stub length reaches 17.5 mm and 20 mm, the frequency shift is much more apparent and second resonances start to occur at higher frequencies. With the shift in operating frequency, the antenna becomes mismatched as depicted in the gradual increase of the VSWR in Figure 17. To retune the antenna, the length of the microstrip feedline is adjusted (Table 3). When retuning the antenna with the microstrip feedline, some cases resulted in improved voltage standing wave ratios that were better than the original patch antenna design. The general relationship is that when the length of the tuning stub is increased, the microstrip feedline is increased to retune the antenna. For the cases in which the frequency shift is much greater, the voltage standing wave ratios could be tuned to only a certain point. This is particularly apparent when the stub length reaches 20 mm. A microstrip feedline length of 63 mm retunes the antenna from a VSWR of 4.45 to 2.22. However, a typical standard for an antenna is to operate with a VSWR below 2. Increasing the microstrip feedline length beyond 63 mm resulted in an increase in VSWR due to some unexpected antenna behaviors.

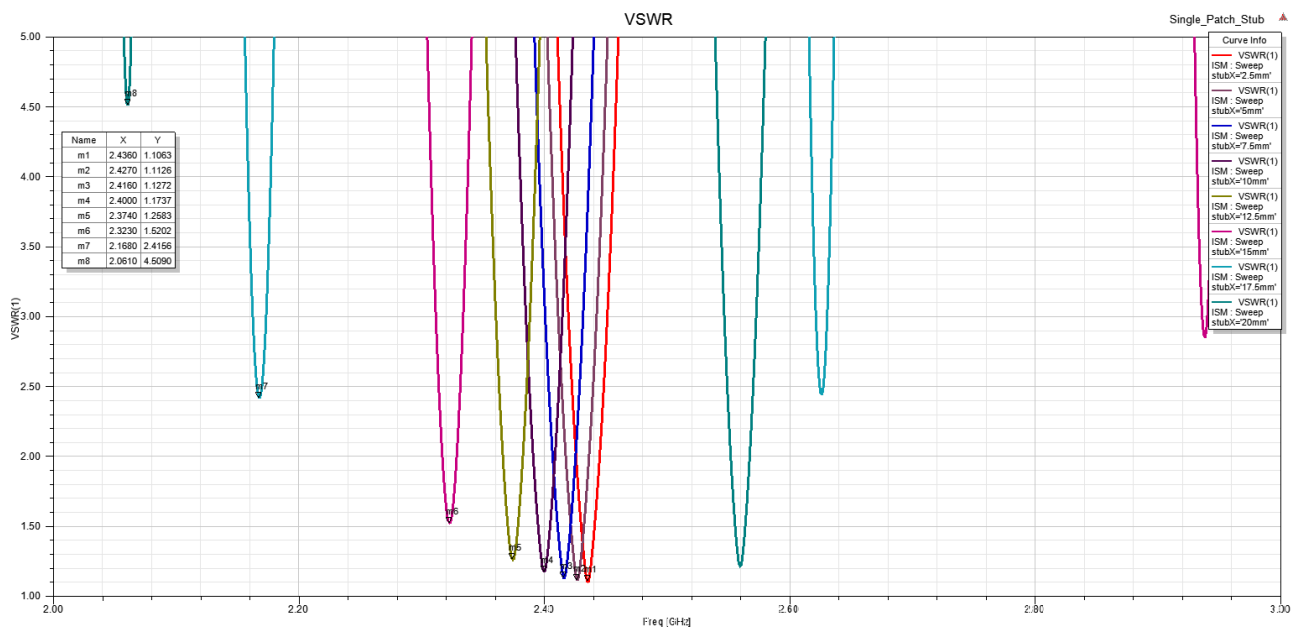


Figure 17. ANSYS results for single patch frequency with stubs

Table 3. Single patch frequency tuning values

Stub Length (mm)	Detuned VSWR	Operating Frequency (GHz)	Microstrip Feedline Length (mm)	Retuned VSWR
0	1.07	2.442	53	Not applicable
2.5	1.10	2.436	54.5	1.08
5	1.11	2.427	54.5	1.07
7.5	1.12	2.416	54.5	1.04
10	1.17	2.4	54.5	1.039
12.5	1.25	2.374	55	1.02
15	1.52	2.323	55.5	1.032
17.5	2.41	2.168	62.5	1.25
20	4.50	2.061	63	2.22

Figure 18 illustrates the combined frequencies on a smith chart. Each point represents the impedance at a certain operating frequency for each stub length. The red dots represent the detuning of the antenna when the stub length is varied from 0 mm to 20 mm. The blue dots represent the retuning of the antenna when the microstrip feedline length is adjusted. Most of the frequencies are retuned successfully to the center of the smith chart, where most of the power is radiated with the exception of the 20 mm stub.

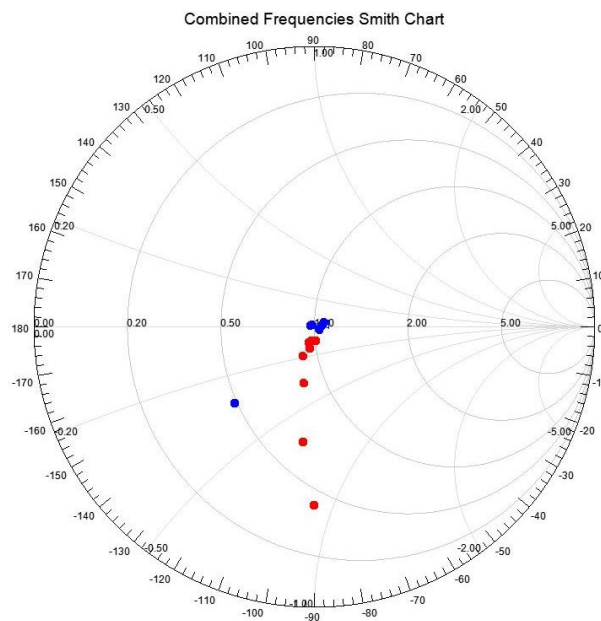


Figure 18. Smith chart illustration of frequency tuning

CHAPTER IV

RESULTS

The fabricated antenna depicted in Figures 19 and 20 is measured using a vector network analyzer and anechoic chamber. The VNA measures the impedance of the antenna, s-parameters, and the voltage standing wave ratio at a specific operating frequency. The impedance, VSWR, and operating frequency results of the fabricated antenna are tabulated in Table 4.



Figure 19. Top side of fabricated antenna



Figure 20. Bottom side of fabricated antenna

Table 4. Simulation and measured values of the fabricated antenna and adjusted antenna

	Operating Frequency	Impedance	VSWR
Measured Values	2.52 GHz	58 Ω	1.22
	2.4 GHz	74 Ω	1.52
Simulated Values	2.4 GHz	53.5 Ω	1.07

The expected operating frequency was 2.4 GHz; however, the fabricated antenna operates at a slightly higher frequency of 2.52 GHz. The operating frequency of the fabricated antenna deviated from the ANSYS design by approximately 0.1 GHz but remains well-matched at a VSWR of 1.22. This is likely due to small inaccuracies in the milling process of the length of the patch antenna. From the parametric studies on microstrip patch antennas, increases in the length of the patch have an inverse effect on the operating frequency. Therefore, to make a comparison of the fabricated antenna to the original ANSYS design at 2.4 GHz, the length of the patch was adjusted by using copper tape. The addition of copper tape increases the patch length which decreases the operating frequency (Figure 21). Measurements for the adjusted fabricated antenna are tabulated in Table 4.

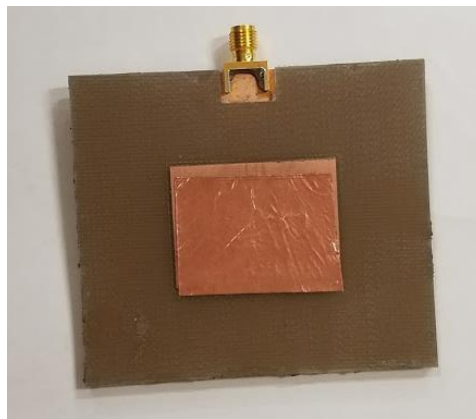


Figure 21. Fabricated antenna with copper tape

The results depicted in Table 4 of the adjusted fabricated antenna show that the operating frequency could be easily altered with the addition of copper tape to the patch antenna. However, this also affects the impedance matching and VSWR. As expected, a higher VSWR results in a higher impedance mismatch. In Table 4, a VSWR of 1.07 corresponds to an impedance match of 53.5 ohms. In comparison, a VSWR of 1.52 corresponds to an impedance mismatch at 74 ohms. The increase in impedance mismatch may be a result of inaccuracies in connections and measurements when using copper tape. Better results could be obtained by refabricating the antenna on the milling machine.

Radiation patterns

The electric and magnetic field radiation patterns of the fabricated antenna and adjusted antenna are measured in the anechoic chamber room depicted in Figure 22. The cones in the chamber room completely absorb electromagnetic waves to reduce reflections and measurement errors in the radiation patterns. The anechoic chamber is used to measure the polarization, beam width, and gain. Since the anechoic chamber has the capability to measure a maximum of two planes at a time, a total of four separate tests were done. To obtain the electric field and electric cross field, the fabricated antenna is secured onto a stand and connected through the feed point. The fabricated antenna transmits a signal, and on the opposite side of the room is a receiver (Figure 22). The stand for the transmitting antenna is attached to a rotating platform which rotates 360 degrees. While the platform rotates 360 degrees, the receiver collects data simultaneously. When the data collection is finished, the fabricated antenna is turned 90 degrees and the procedure is repeated to measure the magnetic field and magnetic cross field. The two tests were performed again for the adjusted antenna, for a total of four separate tests.

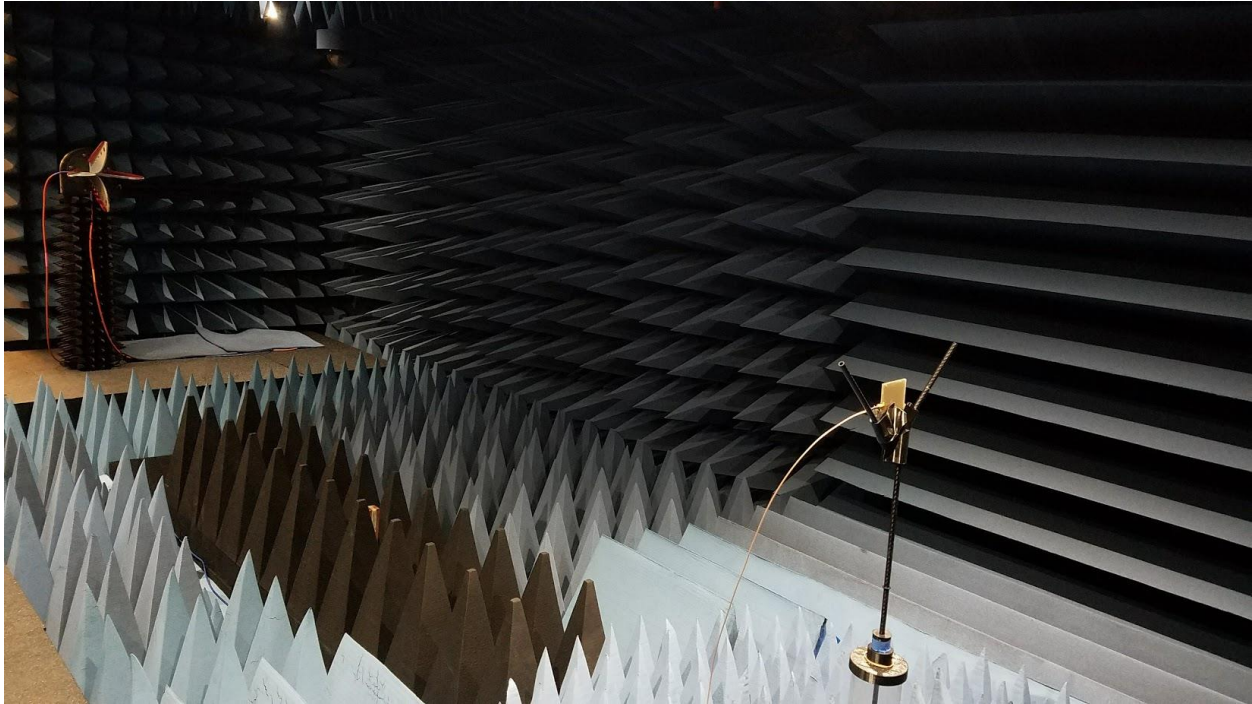


Figure 22. Antenna set up in the anechoic chamber

The simulated gain on ANSYS is approximately 3 dB gain. The aperture coupled microstrip patch antenna is linearly polarized. Figures 23 and 24 show the plotted results of the fabricated antenna which operates at 2.5 GHz. The magnetic field pattern is not as consistent as the electric field pattern (Figures 23 and 24).

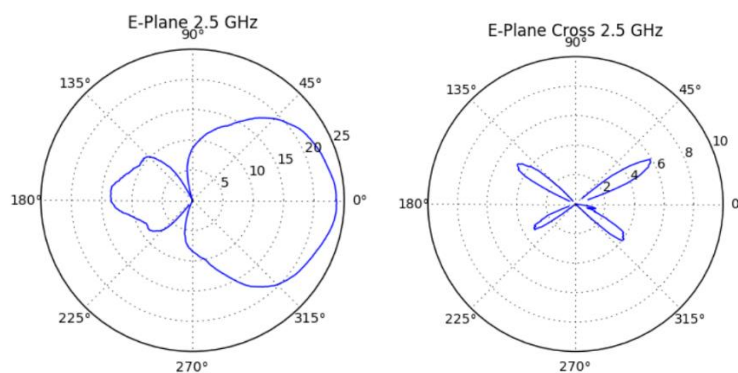


Figure 23. E-plane and E-plane cross for antenna design at 2.5 GHz

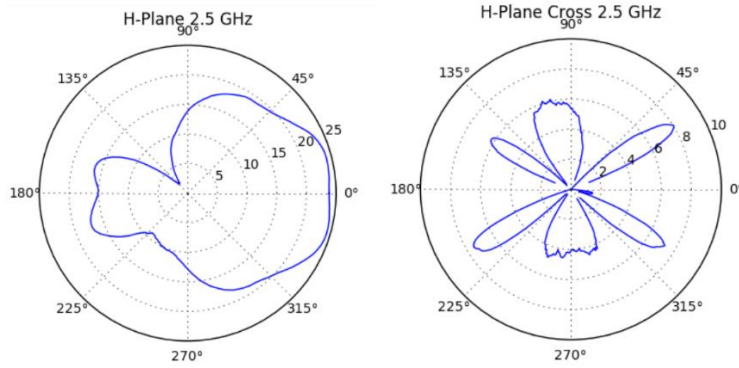


Figure 24. H-plane and H-plane cross for antenna design at 2.5 GHz

Figures 25 and 26 show the results of the adjusted antenna at 2.4 GHz. For comparison, the plots are superimposed with the ANSYS radiation pattern simulations which are depicted in green. When the radiation patterns are plotted together, the results show that the experimental electric and magnetic field patterns fall within the simulations, and also exhibit some back radiation.

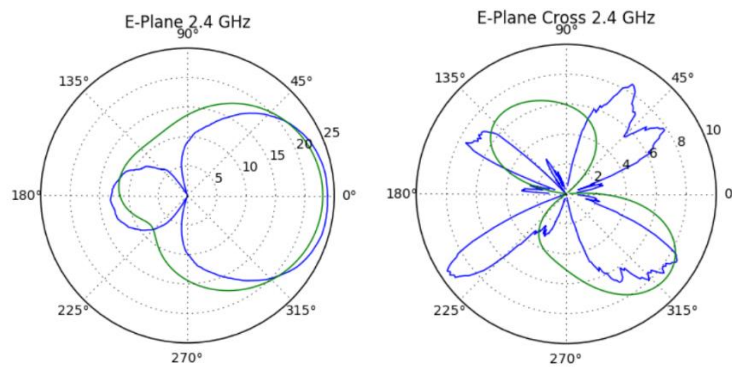


Figure 25. E-plane and E-plane cross for antenna design at 2.4 GHz

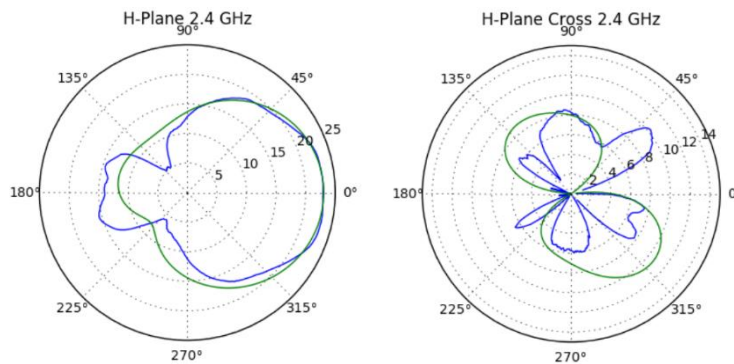


Figure 26. H-plane and H-plane cross for antenna design at 2.4 GHz

CHAPTER V

CONCLUSION

Summary

This research paper presents a method to design an aperture coupled microstrip patch antenna and an exploration of reconfiguration methods to tune an antenna. A parametric study shows the effects of the various parameters in designing an aperture coupled microstrip patch antenna. Two different antenna designs are presented in this paper. One designed on FR4 epoxy was fabricated and resulted in behaviors that did not deviate far from the expected performance on ANSYS. The other antenna design on Rogers AD250C was used to gain insight on tuning the antenna by using stubs. With these two antenna designs, the outcomes of this research are a fabricated antenna with agreement among the simulated and experimental results, and positive results in simulating the frequency reconfiguration of an aperture coupled microstrip patch antenna.

Future work

Future work that would extend this research topic include implementing reconfiguration mechanisms (RF MEMS, RF PIN diodes, and varactors) to the aperture coupled microstrip patch designs presented in this research paper. For example, the variable capacitor can be combined with the injection of liquid metal into the antenna for continuous frequency tuning. Performance of a thorough study on the comparisons of different reconfiguration methods for aperture coupled microstrip patches can lead to an optimal solution for easy implementation of a reconfigurable antenna in a structural composite.

REFERENCES

- [1] Bernhard, J. T. (2007). *Reconfigurable antennas*. S.l.: Morgan and Claypool.

- [2] Civerolo, M. (2010). *Aperture Coupled Microstrip Antenna Design and Analysis*. California Polytechnic State University.

- [3] Civerolo, M. (2011). Aperture Coupled Patch Antenna Design Methods. 876-879.

- [4] Costantine, J., Tawk, Y., Barbin, S. E., & Christodoulou, C. G. (2013, March). Reconfigurable Antennas: Design and Applications. *Proceedings of the IEEE Vol. 103, No. 3*, 424-437.

- [5] How and Why to Use PIN Diodes for RF Switching. (2016, December 28). Retrieved April 08, 2018, from <https://www.digikey.com/en/articles/techzone/2016/dec/how-and-why-to-use-pin-diodes-for-rf-switching>

- [6] Iseri, Kadri. (2012). *Analysis of Dual-Polarized Aperture-Coupled Microstrip Antennas with H-Shaped Slots and Equivalent Circuit Modeling of H-Shaped Slots (master's thesis)*. Middle East Technical University

- [7] Pozar, D. M. (1996, May). *A Review of Aperture Coupled Microstrip Antennas: History, Operation, Development, and Applications*. Massachusetts, Amherst.

- [8] S K, L., H, S., & A, K. (2009). RF MEMS SWITCH: An overview at-a-glance. Retrieved April 08, 2018, from <http://ieeexplore.ieee.org/stamp/stamp.jsp?tp=&arnumber=5407222>

APPENDIX

Python code for plotting radiation patterns

```
from pylab import *
import numpy as np
import matplotlib.pyplot as plt
import pandas as pd

#import excel data files
data1 = pd.read_excel(open('data.xlsx','rb'), sheetname='E-Plane 2.4 Ghz')
data2 = pd.read_excel(open('data.xlsx','rb'), sheetname='H-Plane 2.4 Ghz')
data3 = pd.read_excel(open('data.xlsx','rb'), sheetname='E-Plane 2.5 Ghz')
data4 = pd.read_excel(open('data.xlsx','rb'), sheetname='H-Plane 2.5 Ghz')

#transpose the data and store data in an array
d1 = np.transpose(data1.as_matrix())
d2 = np.transpose(data2.as_matrix())
d3 = np.transpose(data3.as_matrix())
d4 = np.transpose(data4.as_matrix())

#import simulation excel files
sim1 = pd.read_excel(open('EPlane.xlsx','rb'))
sim2 = pd.read_excel(open('HPlane.xlsx','rb'))

#store data in arrays
s1 = sim1.as_matrix()
s2 = sim2.as_matrix()

theta = np.arange(0, 361, 1)
theta = (theta * np.pi)/180

#plot polar graphs using scaling factors
plt.polar(theta, d1[:,0]+7)
plt.polar((s1[:,0]*np.pi)/180, s1[:,1]+50)
plt.title('E-Plane Cross 2.4 GHz')
plt.show()

plt.polar(theta, d1[:,1])
plt.polar((s1[:,0]*np.pi)/180, s1[:,2]+20)
plt.title('E-Plane 2.4 GHz')
plt.show()

plt.polar(theta, d2[:,0])
plt.polar((s1[:,0]*np.pi)/180, s1[:,1]+52)
plt.title('H-Plane Cross 2.4 GHz')
plt.show()
```